

Symmetry-broken silicon disk array as an efficient terahertz switch working with ultra-low optical pump power*

Zhanghua Han(韩张华)^{1,†}, Hui Jiang(姜辉)¹, Zhiyong Tan(谭智勇)^{2,3},
Juncheng Cao(曹俊诚)^{2,3}, and Yangjian Cai(蔡阳健)¹

¹ Shandong Provincial Key Laboratory of Optics and Photonic Devices, School of Physics and Electronics, Shandong Normal University, Jinan 250358, China

² Key Laboratory of Terahertz Solid-State Technology, Shanghai Institute of Microsystems and Information Technology, Chinese Academy of Sciences, Shanghai 200050, China

³ Center of Materials Science and Optoelectronics Engineering, University of Chinese Academy of Sciences, Beijing 100049, China

(Received 30 March 2020; revised manuscript received 21 May 2020; accepted manuscript online 12 June 2020)

The advancement of terahertz technology in recent years and its applications in various fields lead to an urgent need for functional terahertz components, among which a terahertz switch is one example of the most importance because it provides an effective interface between terahertz signals and information in another physical quantity. To date many types of terahertz switches have been investigated mainly in the form of metamaterials made from metallic structures and optically-active medium. However, these reported terahertz switches usually suffer from an inferior performance, e.g., requiring a high pump laser power density due to a low quality factor of the metallic metamaterial resonances. In this paper, we report and numerically investigate a symmetry-broken silicon disk based terahertz resonator array which exhibits one resonance with ultrahigh quality factor for normal incidence of the terahertz radiations. This resonance, which can never be excited for regular circular Si disks, can help to realize a superior terahertz switch with which only an ultra-low optical pump power density is required to modify the free carrier concentration in Si and its refractive index in the terahertz band. Our findings demonstrate that to realize a high terahertz transmittance change from 0 to above 50%, the required optical pump power density is more than 3 orders of magnitude smaller than that required for a split-ring resonator (SRR) based terahertz switch reported in the literature.

Keywords: silicon disk, symmetry-broken, terahertz switch, photocarrier, bound state in continuum

PACS: 42.60.Da, 42.79.Ta, 87.50.U–

DOI: 10.1088/1674-1056/ab9c0b

Recent years have seen the advancing of terahertz (THz) technology and its applications in a variety of areas, among which typical examples include substance identification^[1] thanks to the unique absorption characteristics of different substances in this spectral band, and THz communications^{[2][3]} making use of the large transmission capacity provided by the high carrier frequency. In particular, the spectrum and frequencies in current 5-generation (5G) communication systems have been extended to the order of a few 10 GHz and will soon enter the true THz regime. From the fundamental point of view, it will be of great importance to investigate functional terahertz components for the THz communications. One essential component in the THz communication system is a terahertz switch (for digital signals) or modulator (for analog signals), which will control the power level of the terahertz output by an external signal. A THz switch is important because it will load the information onto the THz signal and then provide an interface between THz radiations and signals in another form, e.g., electrical or optical. Researchers have made some endeavors to realize some THz

switching components in recent years and the main challenge is still to find a material or a structure whose characteristic is highly sensitive to the external conditions.^[4] VO₂ as an active material can be used for efficient THz switching^[5] because of its unusual phase transition from insulating state to conductive one when the temperature changes over a threshold of moderate value. Unfortunately, like many thermo-optical devices, the response time is an unsolved issue, which restricts the application of this device in high speed networks. Chen *et al.*^[6,7] have made use of a metallic material in the form of split-ring resonators (SRR) for efficient terahertz switching. By using the large dependence of the SRR resonances on the property of the semiconductor materials filled into the SRR slits, they have experimentally demonstrated THz switching using an electrical gating^[6] or optical pumping.^[7] Some people also made use of this scheme of active tuning of semiconductor properties with optical pumping to realize an active control of electromagnetically induced transparency analogue in terahertz metamaterials.^[8] Due to the small thickness of the metallic constituent, the active medium of the semiconductor

*Project supported by the National Key R&D Program of China (Grant No. 2017YFA0701005) and the National Natural Science Foundation of China (Grant Nos. 11974221, 91750201, 61927813, and 61775229). Z. Han also acknowledges the support from the Taishan Scholar Program of Shandong Province, China (Grant No. tsqn201909079) and Zhejiang Provincial Natural Science Foundation of China (Grant No. LY15F050008).

†Corresponding author. E-mail: zhan@sdnu.edu.cn

© 2020 Chinese Physical Society and IOP Publishing Ltd

<http://iopscience.iop.org/cpb> <http://cpb.iphy.ac.cn>

also has a low volume. Furthermore, the semiconductor materials usually have a large refractive index and then deteriorate the quality factors of the SRR resonances. As a result of both effects, an evident modulation of THz transmission usually requires a large gating voltage or high optical pump power. For example, for the tuning of the THz transmission through the metamaterial by more than 50%, the required pump laser power to cover a sample with the diameter around 1 cm will be around 500 mW,^[7] which is far beyond the typical laser powers in practical optical communication networks.

In this paper, we demonstrate a new non-metallic scheme for highly-efficient THz switching based on the optical pump. This scheme is based on a novel resonance supported by the symmetry-broken Si disk array. Different with the widely investigated electric or magnetic dipole modes^[9] supported by high-index nanodisks in the optical regimes, this novel resonance has a much larger quality factor. As a result, the THz transmittance at resonance is highly sensitive to the refractive index of the Si material in the THz band, which can be easily controlled by tuning the free carrier density using the optical pump method. Using the experimental result of the dependence of Si photocarrier density on the pump power density in Ref. [7] as a reference, our results demonstrate that to achieve a THz transmittance change from 0 to above 50%, the required pump laser power at 800 nm is more than 3 order of magnitude smaller than that used for the SRR based metamaterial THz switch.

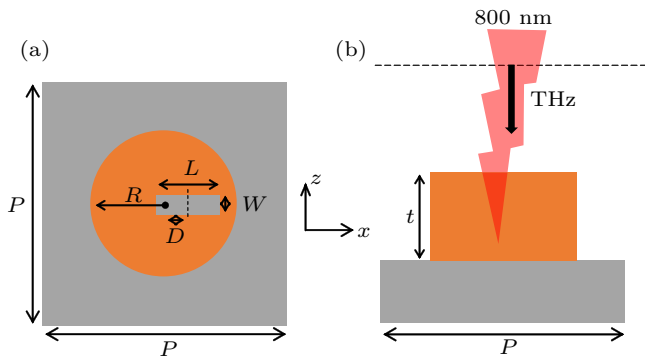


Fig. 1. (a) Top view of one unit cell of the symmetry-broken Si disk array used for THz switching. (b) Cross-sectional view of the investigated structure. The black arrow indicates the THz radiation while the lightning symbol stands for the optical pump.

Our investigated structure is schematically illustrated in Fig. 1. The Si circular disk with radius $R = 42 \mu\text{m}$ and thickness $t = 40 \mu\text{m}$ is located upon a polymer substrate whose refractive index is assumed as 1.5 in the THz frequencies. The polymer is used only as a substrate to support the Si disks and it can be combined with the Si using the bonding process. A narrow rectangular air slot with the dimension of $L = 24 \mu\text{m}$ by $W = 4 \mu\text{m}$ is located on one side of the Si disk and etched through it to the bottom, resulting in the name of the whole structure as symmetry-broken Si disk. Note that the slot may

not start from the center of the disk. In this paper, we assume the distance D between the disk center and the center of the slot to be $8 \mu\text{m}$. The periodicity of the array along both directions is set to $120 \mu\text{m}$, ensuring a subwavelength operation in the frequency band of our interest.

The solid line in Fig. 2(a) gives the calculated transmission spectrum of THz radiations propagating normally through the structure. A plane THz wave polarized along y -direction is used as the excitation in the simulations based on the finite element method. In addition to a broad resonance at around 1.45 THz in the high-frequency region, an ultra-sharp resonance at 1.143 THz is observed, which has an evident profile of the Fano type. For comparison, we have also given (the black dotted line in Fig. 2(a)) the transmission spectrum for the same excitation through a reference sample of pure solid Si disk array, i.e., no air slot in the disk. One can see that a similar transmission dip with comparable bandwidth as the broad resonance in our structure is present for the reference sample. It is known that these wavelength-scale disks made from high index dielectrics support multipole resonances, e.g., electric and magnetic dipoles,^[10] and these resonances have been utilized to enhance the light–matter interactions and nonlinear applications.^[11] The transmission dip for both the reference sample and the broad resonance in our structure is attributed to this kind of resonance, and the mismatch between the two dips is due to an effective optical path change when the air slot is present. Our simulation results also reveal that these two resonances belong to the type of electric dipole resonance.

The narrow resonance in the lower part of the spectrum is of more interest because it has a much narrower bandwidth. Figure 2(b) shows an enlarged part of it close to the resonance. It is clearer now that this resonance has a bandwidth around 0.5 GHz, suggesting that this resonance has a quality factor larger than 2200. To the best of the authors' knowledge, this is the highest quality factor that one has observed in the THz metamaterials with subwavelength dimension of the unit cell. It is worth noting that the quality factor can be further improved by adjusting the dimension and lateral position of the air slot. To study the origin of this resonance, we plot in Fig. 2(c) the magnetic field as well as the vectorial distribution of the electric field across the central plane of the Si disk at the resonance of 1.143 THz. It is quite clear that the electric field forms a perfect circulation and the magnetic field is the strongest in the center. These field distributions show that the sharp resonance is a magnetic dipole resonance. However, the magnetic dipole momentum is along z direction, which is perpendicular to the magnetic field of the incident THz plane wave. So an overlap of 0 between the magnetic fields is achieved when a plane wave is normally incident onto the structure. That explains why this sharp resonance cannot be excited in the reference sample. When the air slot is present

inside the Si disk, the THz plane wave with y -polarization first excites a strong electric field inside the slot. One can see in Fig. 2(c) that the electric field is stronger inside the air slot than elsewhere. Because the electric field lines in the slot have a large overlap with those circulating in the Si disk, the resonance at 1.143 THz is subsequently excited. The field distributions in Fig. 2(c) also reveals that one needs to adjust the relative position of the air slot inside the disk to tune the coupling between the incoming radiation and the local field in order to achieve a resonance with an even higher quality factor.

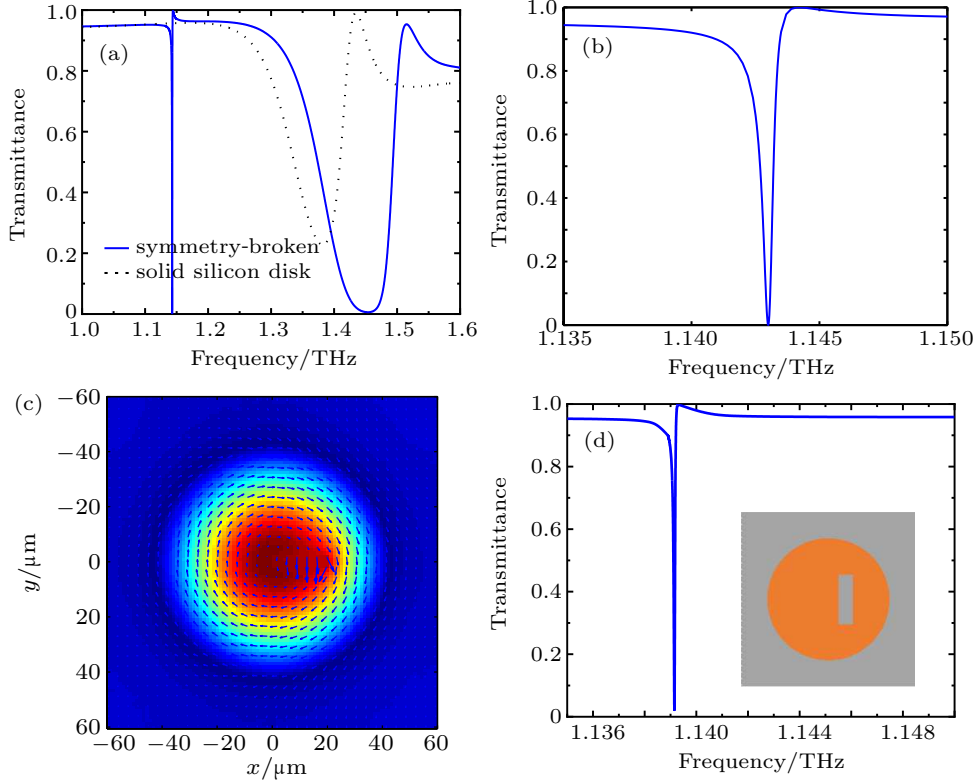


Fig. 2. (a) The solid blue line represents numerically calculated transmission spectrum for THz radiations normally propagating through the symmetry-broken Si disk array, while the dotted line is for the spectrum through a solid Si disk array for comparison. (b) An enlarged part of the transmission spectrum close to the sharp resonance. (c) Magnitude profile for the magnetic field (Hz) and the vectorial distribution for the electric field. (d) Transmission spectrum when the air slot is rotated by 90° while keeping its center unchanged. The inset illustrates the geometry.

To gain more insight into the physical mechanism of the high Q factor, we solve for the eigen frequencies for the unit cell. In the calculations, Floquet periodic boundary conditions of $k_x = k_y = 0$ are used, which correspond to the normal incidence of terahertz waves as is used in the transmission spectrum calculations. The results for the calculated eigen frequencies and the corresponding quality factors are presented in Fig. 3 for two cases: (1) The length of the air slot L is kept at 24 μm while the width W shrinks from 5 μm to 1 μm ; (2) W is fixed at 4 μm and L increases from 16 μm to 32 μm . In both cases, the center of the air slot remains the same, i.e., the value of D is constantly 8 μm . From the results one can see the general trend is that when the air slot shrinks in area size, the eigen frequency remains weakly affected with only a slight decrease. However, the Q factor increases substantially and can easily reach a value above 10^5 when the area size is smaller than 24 $\mu\text{m} \times 1 \mu\text{m}$. Detailed calculation results show that the eigenvalue is above the light dispersive curve in air, implying that the physical origin of the high Q resonance stems from a bound state in continuum (BIC).^[12,13] A Si disk with no defect

supports the BIC mode with infinite Q factor, which, however, cannot be excited. A defect in the disk in the form of an air slot can work as a perturbation and changes the BIC into a quasi-BIC mode which has a finite yet high Q factor and can be easily excited at normal incidence. This explains why the Q factor is higher at smaller slot areas. A small perturbation to the original BIC mode whose profile is shown in Fig. 2(c) will also help to achieve a higher Q factor. An example is shown in Fig. 2(d), in which the air slot is rotated by 90° while its center is kept the same. Apparently one can see in the transmission spectrum that a resonance with a much higher Q value compared to that in Fig. 2(b) is present now due to a weaker interference between the air slot mode and the BIC mode in the Si disk. One can also decrease the value of D so that the center of the air slot moves towards that of the disk to have a smaller perturbation. In that case the quasi-BIC mode will be closer to the real BIC mode and the Q factor will see a significant increase. We also note that in all the above calculations, the results are polarization dependent because one needs to excite the mode in the air slot first as a perturbation for the BIC

mode. Due to the asymmetry of the air slot, a different incident polarization will not excite the quasi-BIC mode at the same spectral region.

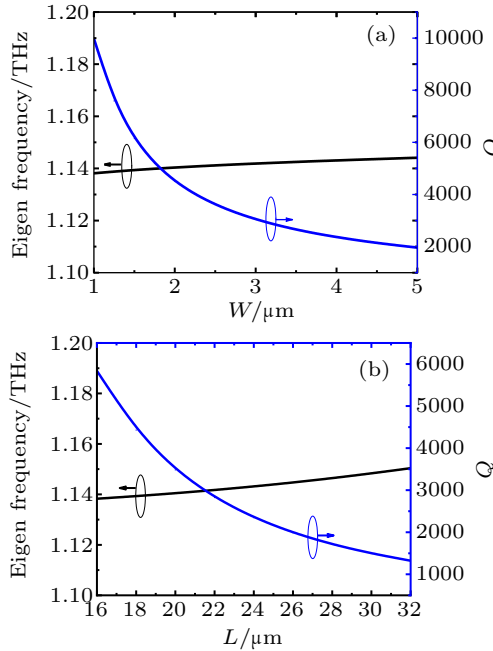


Fig. 3. Numerically calculated eigen frequencies of the unit cell when the horizontal wave vectors are set as $k_x = k_y = 0$ for different geometry parameters: (a) L is fixed at 24 μm while W changes; (b) W is fixed at 4 μm while L changes.

The high-quality factor indicates that the spectral position of this resonance is highly sensitive to the refractive index of the disk constituent material. The shift of resonance will result in a pronounced change of transmittance at the original frequency, which suggests that this structure can work as an efficient THz switch. We further demonstrate this application using the optical pump approach, making use of the fact that the photon-generated carrier will further lead to a change of the Si index in the THz band.

A pump laser at the wavelength of 800 nm is used. Since this value is much smaller than those dimensions in our structure, we ignore the diffraction of laser at the slot and disk edges for simplicity. Different with the case using the SRR structures^[7] where the Si is very thin (600 nm) and the pump laser intensity as well as the photo-excited carriers can be considered as uniform therein, here we have to consider the propagation and decaying of laser in the whole thickness of the Si layer. We assume the same internal quantum efficiency for different power level of the laser. Although the quantum efficiency may have some dependence on the pump power level, this assumption is still valid in our case where the overall pump laser power density is low. Then the photocarrier concentration will be

$$n(z) = n_0 e^{-2n_2 k_0 (-z+r)}, \quad (1)$$

where n_0 is the photocarrier density at the top surface of the Si disk, n_2 is imaginary part of the Si index at the pump

wavelength of 800 nm and is found to be 0.0065435,^[14] k_0 is the wave-number of the pump laser in vacuum. By using a similar way as for highly doped Si for THz absorbing applications,^[15,16] the induced Si index in the THz band can be determined by the Drude equation

$$\epsilon_{\text{Si}} = \epsilon_{\infty} - \frac{\omega_p^2}{\omega(\omega + j\gamma)}, \quad (2)$$

where $\epsilon_{\infty} = 11.7$ is the permittivity of intrinsic Si, and ω is the THz angular frequency. The position dependent plasma frequency $\omega_p(z)$ and the damping rate $\gamma(z)$ are related with the free carrier concentration by the following equations:

$$\omega_p^2(z) = \frac{e^2 n(z)}{m^* \epsilon_0}, \quad (3)$$

$$\gamma(z) = \frac{e}{m^* \mu(z)}, \quad (4)$$

where e is the electron charge, m^* is the effective mass of free carrier (for electrons, $m^* = 0.26 m_0$ with m_0 being the stationary mass of electron), $\mu(z)$ is the free carrier mobility and calculated by the following empirical formula:

$$\mu(z) = \mu_{\min} + \frac{\mu_{\max} - \mu_{\min}}{1 + (n(z)/n_{\text{ref}})^{\alpha}}. \quad (5)$$

The empirical parameters of μ_{\min} , μ_{\max} , and α in Eq. (5) are chosen as 65 $\text{cm}^2/\text{V}\cdot\text{s}$, 1330 $\text{cm}^2/\text{V}\cdot\text{s}$, $8.5 \times 10^{16} \text{ cm}^{-3}$, and 0.72 for Si working at room temperature^[17] in our calculations.

For a fair comparison, we use the same values of the photocarrier density and the pump laser power as in Ref. [7], i.e., a pump laser power of 500 mW on a 1 cm-diameter circle will induce a photocarrier density of $n_0 = 2.5 \times 10^{18} \text{ cm}^{-3}$. In other words, a pump power density of 637 mW/cm² corresponds to a photocarrier density of n_0 . Using a linear dependence of n_0 on the laser power and combining Eq. (1), one can calculate the photocarrier density along z direction inside the Si disk and the induced change of the Si refractive index in the THz frequencies. Note that a plane wave of the pump laser is assumed to be incident onto the sample, so the laser power density is the same over the whole sample surface.

As a typical example, the red line in Fig. 4 presents the photocarrier density along the thickness of the Si layer at a quite low pump lower density of 76 $\mu\text{W}/\text{cm}^2$. A photocarrier density as high as $3.0 \times 10^{14} \text{ cm}^{-3}$ is excited on the top surface of the Si disk array and it decays to the bottom following the behavior of the pump laser attenuation. As a result of these photocarriers, a slight change of Si index in the THz frequencies is seen as shown by the solid black line in Fig. 4, reduced from original 3.418 to 3.411 on the disk surface. It is also observed that the change of the Si index is not uniform through the thickness of the Si layer, with negligible change at the bottom. Thanks to the large quality factor associated

with the symmetry-broken Si disk array, the slight and even non-uniform change of the Si index still leads to a pronounced shift of the resonance.

For the switching application, we use $f_0 = 1.143$ THz at the original resonance as the working frequency and monitor its transmittance while changing the power of the incident pump laser. The dependence of the transmittance at this frequency is found to be highly dependent on the pump laser power and an increase of the transmittance from 0 to above 50% occurs even when the pump laser is only at a few tens of μW level, see Fig. 5(a). The increase of transmittance saturates around 80%. This is because the presence of photo-carriers will lead to a decrease in the Si index and a subsequent blue-shift of the resonance. Figure 5(b) presents a comparison of the transmission spectrum around the resonance between two cases when there is no pump and when the laser power density is $127 \mu\text{W}/\text{cm}^2$. A clear blue-shift and an increase of the transmittance at 1.143 THz are seen. The decrease in transmittance on resonance in the two cases is attributed to a change of the forward scattering cross section of these resonators when the Si index decreases. As is shown in Fig. 5(b), the resonance has a Fano profile and the transmittance on the left of the resonance is lower than unity. One can also choose another working frequency $f_0 = 1.144$ THz which is located on the right side of the resonance with a transmittance of 100%. When the optical pump laser is present, the resonance experiences a blue-shift and a transmittance change from 100% to a lower value can be expected.

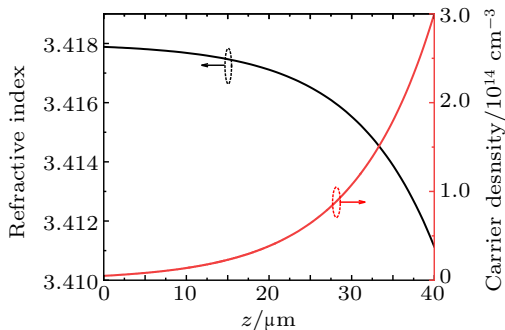


Fig. 4. Photocarrier density at the pump laser power density of $76 \mu\text{W}/\text{cm}^2$ and the corresponding Si refractive index (real part) along the thickness of the Si layer. $z = 0$ is the bottom of the Si layer.

One possible drawback with Si based components for switching might be from the low mobility of electrons in Si. Nevertheless, for really high-speed applications, one can replace Si with other III-V materials like GaAs which has both large refractive index in the THz frequencies and high photocarrier mobility. Then both high switching efficiency and extremely short response time can be achieved. Another issue we need to discuss is related with the thermal dependence of Si refractive index in the THz region. Although the Si thermo-optic coefficient is low, however, a change in the temperature will still lead to some variations in the Si refractive

index in the THz band and a subsequent spectral shift of the high Q resonance. If we use the Si thermo-optic coefficient $dn/dT = 1.8 \times 10^{-4} \text{ K}^{-1}$ ^[18] at 300 K, our calculations find that the transmittance at the resonance around 1.1431 THz will increase from 0 to 0.05. Nowadays it is pretty convenient to keep the temperature stability at an accuracy of 0.1°C , so thermal stability can be maintained using a temperature controller.

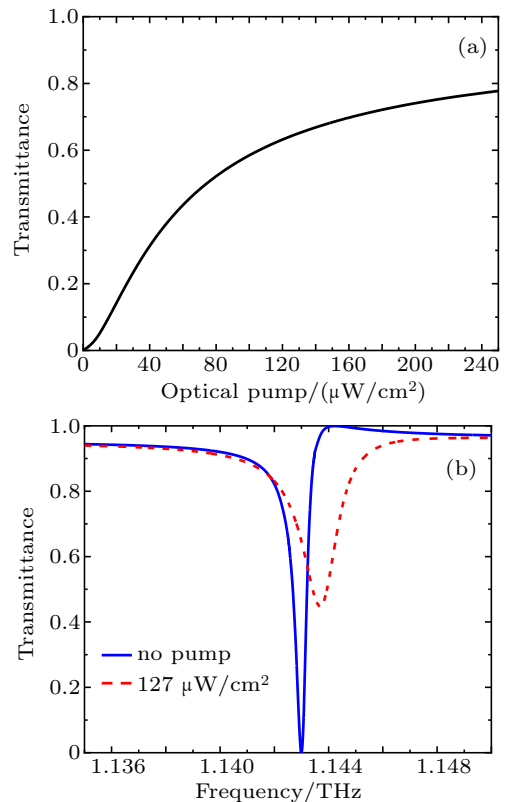


Fig. 5. (a) Transmittance at 1.143 THz at different power of the pump laser. (b) Transmission spectrum for two cases, when there is no pump laser (blue solid line) and when the pump laser power density is $127 \mu\text{W}/\text{cm}^2$ (red dashed line).

In summary, we have demonstrated the efficient THz switching using the symmetry-broken Si disk structures and the optical pump method. The high quality factor of the resonance associated with this structure renders it possible to realize a switching of THz transmittance from 0 to above 50% with a pump laser power density as low as the level of $100 \mu\text{W}/\text{cm}^2$ to slightly modify the Si photocarrier density and the induced Si index in the THz frequencies. This pump laser power density level is more than 3 orders of magnitude smaller than that used for the SRR-based THz switches reported in the literature. A low pump laser power is essential for practical applications in coherent THz communication systems, because one needs to up-convert the laser in an optical telecommunication network to be above the semiconductor band-gap for photoexcitation. Considering this effect, we believe our structure, as an supplement to terahertz switches in other forms,^[19,20] is superior over SRR based counterparts and holds the promise to realize a combination between optical and the THz com-

ponents and achieve a seamless integration between the two networks.

References

- [1] Bigourd D, Cuisset A, Hindle F, Matton S, Fertein E, Bocquet R and Mouret G 2006 *Opt. Lett.* **31** 2356
- [2] Nagatsuma T, Ducournau G and Renaud C C 2016 *Nat. Photon.* **10** 371
- [3] Ma J, Karl N J, Bretin S, Ducournau G and Mittleman D M 2017 *Nat. Commun.* **8** 1
- [4] Chanana A, Liu X, Zhang C, Vardeny Z V and Nahata A 2018 *Sci. Adv.* **4** eaar7353
- [5] Seo M, Kyoung J, Park H, Koo S, Kim H, Bernien H, Kim B J, Choe J H, Ahn Y H, Kim H, Park N, Park Q, Ahn K and Kim D 2010 *Nano Lett.* **10** 2064
- [6] Chen H, Padilla W J, Zide J M O, Gossard A C, Taylor A J and Averitt R D 2006 *Nature* **444** 597
- [7] Chen H T, O'Hara J F, Azad A K, Taylor A J, Averitt R D, Shrekenhamer D B and Padilla W J 2008 *Nat. Photon.* **2** 295
- [8] Gu J, Singh R, Liu X, Zhang X, Ma Y, Zhang S, Maier S A, Tian Z, Azad A K, Chen H T, Taylor A J, Han J and Zhang W 2012 *Nat. Commun.* **3** 1151
- [9] Kuznetsov A I, Miroshnichenko A E, Brongersma M L, Kivshar Y S, Luk'yanchuk B and Luk B 2016 *Science* **354** aag472
- [10] Sain B, Meier C and Zentgraf T 2019 *Adv. Photon.* **1** 024002
- [11] Liu S, Sinclair M B, Saravi S, Keeler G A, Yang Y, Reno J, Peake G M, Setzpfandt F, Staude I, Pertsch T and Brener I 2016 *Nano Lett.* **16** 5426
- [12] Hsu C W, Zhen B, Stone A D, Joannopoulos J D and Soljacic M 2016 *Nat. Rev. Mater.* **1** 16048
- [13] Koshelev K, Bogdanov A and Kivshar Y 2019 *Sci. Bull.* **64** 836
- [14] Aspnes D E and Studna A A 1983 *Phys. Rev. B* **27** 985
- [15] Zhang Y and Han Z 2015 *AIP Adv.* **5** 017113
- [16] Wang T, Shen S, Liu J, Zhang Y and Han Z 2016 *Opt. Mater. Express* **6** 523
- [17] Caughey D M and Thomas R E 1967 *Proc. IEEE* **55** 2192
- [18] Komma J, Schwarz C, Hofmann G, Heinert D and Nawrodt R 2012 *Appl. Phys. Lett.* **101** 041905
- [19] He X, Lin F, Liu F and Shi W 2020 *J. Phys. D: Appl. Phys.* **53** 155105
- [20] He X, Lin F, Liu F and Zhang H 2020 *Nanomaterials* **10** 39